Journal of Alloys and Compounds 509 (2011) 2833–2837

Contents lists available at ScienceDirect

Journal of Alloys and Compounds

journal homepage: www.elsevier.com/locate/jallcom

Exchange bias behaviour in magnetron sputtered $Ni_{49.8}Mn_{36.1}Sn_{13.9}$ ferromagnetic shape memory alloy thin film

Ritu Vishnoi, Davinder Kaur*

Functional Nanomaterials Research Laboratory, Department of Physics and Center of Nanotechnology, Indian Institute of Technology Roorkee, Roorkee 247667, India

ARTICLE INFO

Article history:
Received 27 June 2010
Received in revised form
12 November 2010
Accepted 19 November 2010
Available online 3 December 2010

Keywords:
Exchange bias
FSMA thin film
DC magnetron sputtering

ABSTRACT

In the present study we report the observation of exchange bias effect in $Ni_{49.8}Mn_{36.1}Sn_{13.9}$ ferromagnetic shape memory alloy thin film, grown on Si (1 0 0) substrate at 550 °C by dc magnetron sputtering. The shift in hysteresis loop up to 41 Oe from the origin was observed at 5 K when film was cooled under a magnetic field of 2 T. Above 55 K, the exchange bias field disappears and the coercivity gets significantly reduced due to the fact that the pinning between an antiferromagnet and ferromagnet becomes weak with increase in temperature. The observed exchange bias behaviour in $Ni_{49.8}Mn_{36.1}Sn_{13.9}$ film is attributed to the presence of AFM–FM interactions that result from the coexistence of antiferromagnetic and ferromagnetic phases in the martensite phase of the film at low temperature. This behaviour is an additional property of the Ni–Mn–Sn thin films apart from various other multifunctional properties.

1. Introduction

Since the discovery of the exchange bias (EB) in 1956 by Meiklejohn and Bean in Co particles embedded in antiferromagnetic CoO [1], the materials exhibiting EB effect have been studied extensively for their potential applications in spin-electronic devices, ultra-high density magnetic recording media [2], sensors, permanent magnets [3,4], giant magnetoresistance and many others. This effect is described as the shift in magnetic hysteresis loop of the material from the origin when it is cooled in the presence of an applied magnetic field. The shift is due to the unidirectional anisotropy produced by the coupling of ferromagnet (FM) to antiferromagnet (AFM) at the interface. Therefore, EB has been observed in systems containing FM/AFM interface, such as AFM–FM bilayers, magnetic nanoparticles [4,5], spin glass systems [3] and thin films [6,7].

One of the promising materials exhibiting EB effect that have attracted increasing attention in recent years are the ferromagnetic shape memory alloys (FSMAs). FSMAs are the interesting materials exhibiting shape memory effect and magnetism simultaneously. They show magnetic field-induced strains at room temperature greater than any magnetostrictive, piezoelectric or electrostrictive material, and faster frequency response than temperature driven shape memory alloys [8]. Among various FSMA materials, Ni–Mn–X (X = In, Sn, Sb) have gained considerable interest due to their multifunctional properties such as shape memory effect, magnetocaloric effect, magnetoresistance, etc., associated with first order martensite to austenite structural transition [9]. Detailed studies on the magnetic and structural properties and EB behaviour of these bulk FSMA materials have been reported [10–16]. However, limited studies have been reported on the growth and magnetic properties of FSMA thin films [17,18]. Thin films of FSMA are important for the applications of these materials in emerging micro-devices such as magnetically driven microelectromechanical systems (MEMS) which require a high quality of FSMA thin films grown on semiconductor substrates [19,20]. To the best of our knowledge, there are no reports on the observation of EB effect in thin films of FSMA, particularly for Ni–Mn–X (X = In, Sn, Sb) system, which is keenly required since most of the device applications based on EB are in thin film form.

In the present study, we report for the first time, as far as we know, the observation of EB effect associated with phase separation in $Ni_{49.8}Mn_{36.1}Sn_{13.9}$ FSMA thin film grown on Si (1 0 0) substrate. It can be useful in technological devices such as read-heads, magnetic sensors or magnetoresistive memories. Precise control of sputtering parameters was done to obtain high quality film. The influence of EB on magnetic properties of the film is investigated in detail.

2. Experimental plan

Ni–Mn–Sn thin film was deposited on (1 0 0) silicon substrate by dc magnetron sputtering system using Ni–Mn–Sn sputtering target of 1 in. diameter and 3 mm thickness. The details of process set up have been described elsewhere [21,22]. The substrates were initially cleaned thoroughly in an ultrasonic bath with a mixture of distilled water and trichloroethylene in 4:1 ratio and then washed with boiled

* Corresponding author at: Department of Physics and Center of Nanotechnology, Indian Institute of Technology Roorkee, Roorkee, India.
Tel.: +91 1332 2285407; fax: +91 1332 273560.
E-mail address: dkaurfph@iitr.ernet.in (D. Kaur).

0925-8388/$ – see front matter © 2010 Elsevier B.V. All rights reserved.
doi:10.1016/j.jallcom.2010.11.133

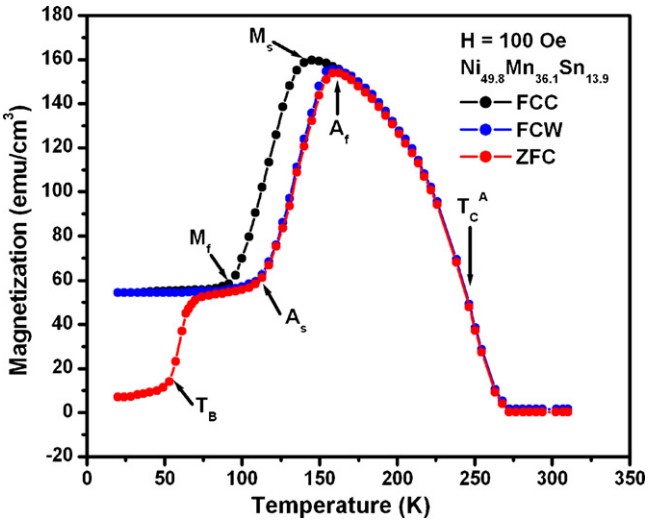

Fig. 1. Zero field cooled (ZFC), field cooled cooling (FCC) and field cooled warming (FCW) magnetization curves as a function of temperature of $Ni_{49.8}Mn_{36.1}Sn_{13.9}$ film obtained at 100 Oe magnetic field.

acetone. Substrate holder was rotated at a speed of 20 rpm in a horizontal plane to achieve a uniform film composition. Before deposition, the chamber was evacuated to a base pressure of the order of 10^{-7} Torr and then backfilled with argon gas to desired pressure of 20 mTorr. The target to substrate distance was fixed at 5 cm. The Ni–Mn–Sn film of ~1 μm thickness was deposited at substrate temperature of 550 °C and fixed sputtering power of 100 W. No post-annealing was performed after deposition. The composition of the film as determined by energy dispersive X-ray analysis (EDAX) is $Ni_{49.8}Mn_{36.1}Sn_{13.9}$.

The orientation and crystallinity of the film was studied using a Bruker AXS D8 advanced diffractometer of CuKα (1.54 Å) radiations in θ–2θ geometry at a scan speed of 1°/min. To obtain a profile fitting with good signal, polycrystalline silicon powder was used for instrumental correction. The film thickness was measured using cross sectional FESEM. The temperature dependence of magnetization $M(T)$ of the film was measured in an external magnetic field (H = 100 Oe) in the temperature range 5 K ≤ T ≤ 310 K using SQUID magnetometer (MPMS, Quantum Design) under zero field cooled (ZFC), field cooled cooling (FCC) and field cooled warming (FCW) modes. The measurements in ZFC mode were taken by first cooling the film from 310 to 5 K in the absence of field and then applying the field and recording the data upto 310 K. Then the film was again cooled to 5 K but this time in the presence of field and the data recorded was in FCC mode. Finally, the temperature was increased to 310 K in the presence of field and measurement obtained was in FCW mode. The magnetization hysteresis loops of the sample were measured after cooling from 310 K to desired temperature, in field ranging from 0.01 to 2 T.

3. Results and discussion

XRD pattern confirmed that the dominant phase of $Ni_{49.8}Mn_{36.1}Sn_{13.9}$ film at room temperature, was austenite and the reflections are indexed to the cubic $L2_1$ structure with lattice parameters, a = 5.954 Å, which agrees with the previously reported value of lattice constant for bulk $Ni_{50}Mn_{36}Sn_{14}$ [12].

Fig. 1 shows the ZFC, FCC and FCW magnetization curves as a function of temperature $M(T)$ of $Ni_{49.8}Mn_{36.1}Sn_{13.9}$ film obtained in a magnetic field of 100 Oe. The area of substrate used for the measurements was 0.5 cm × 0.5 cm. The magnetization data for the film was corrected to account for the diamagnetic contribution of the Si (1 0 0) substrate using equation:

$$M_{\text{film}}(H) = M_{\text{total}}(H) - \chi_{\text{substrate}} \cdot H$$

where, $\chi_{\text{substrate}}$ is the susceptibility of the substrate, M_{total} is the magnetization of (film + substrate), and H is the applied magnetic field. The measured value of susceptibility for Si (1 0 0) substrate comes out to be -5.736×10^{-8}. During FCC, the magnetization rises sharply around 247 K which is due to the paramagnetic (PM) to FM transition in the austenitic state defined as the ferromagnetic Curie temperature (T_C^A) of austenite phase. Below T_C^A, with decrease of temperature, the magnetization first increases to a maximum value and then decreases abruptly at martensite start temperature (M_s) and reaches minimum value at martensite finish temperature (M_f) which is due to first order structural transition from FM austenite to martensite phase. The similar behaviour is observed for the FCW curve however the FCW curve does not retrace the FCC curve but show hysteresis in the temperature range 91–162 K indicating the occurrence of first-order structural transition in the film. The characteristic temperatures of structural transition obtained from FCC and FCW curves are M_s = 139 K, M_f = 91 K, A_s = 112 K and A_f = 162 K, where M_s and M_f are martensite start and finish temperatures and A_s and A_f are austenite start and finish temperatures respectively. The thermal hysteresis between FCC and FCW curves observed during transformation is 18 K. With further decrease of temperature, at around 80 K, the ZFC and FCC curves split showing irreversible behaviour and splitting gets more enhanced with decrease of temperature. This splitting indicates that sample exhibits different magnetic phase during the two measured processes, i.e. ZFC and FCC. The separation between the low field FC and ZFC curves at T_C is often observed in a pure ferromagnetic system due to the pinning of magnetic flux at the defect sites such as grain boundaries and also due to the magnetocrystalline anisotropy. In the present case the splitting occurs in a region of martensite phase much below the T_C of the sample which indicates that pinning of magnetic flux is not the primary reason for the splitting between FC and ZFC curve. It has been shown that in Mn rich Ni–Mn–Sn alloy all the Mn atoms on regular Mn sites have a FM interaction whereas the excess Mn atoms occupying the Sn sites are coupled via AFM interaction to the surrounding Mn atoms on regular Mn sites [10]. The AFM order in $Ni_{50}Mn_{36}Sn_{14}$ was also observed experimentally by neutron diffraction experiments [23]. Also extended X-ray absorption fine structure results reveal that the distance of Mn–Mn between Mn atoms at regular sites and Mn atoms at Sn sites decreases under martensitic transformation from high temperature austenite phase to low temperature martensite phase. This decrease in Mn–Mn distance will also contribute to AFM exchange between them [24]. Furthermore, due to these AFM interactions the FM domains will get themselves pinned in various configurations when system is cooled in presence of field. Therefore, the separation between the ZFC and FCC curves can be understood by considering that two magnetically inhomogeneous phases, FM and AFM, coexist in martensite phase, similar to the artificial FM/AFM bilayer film. But unlike the FM/AFM bilayer system, there is no well defined interface in our case. The coexistence of FM and AFM phases can be explained such that the domains of FM phase are embedded in a matrix which is composed of AFM phase. The ZFC curve of the film shows a sharp decrease in magnetization at around 55 K with decrease in temperature, as the AFM interaction begins to dominate with decreasing temperature. Since the EB effect vanishes above this temperature (discussed later in Fig. 2), it is referred as the EB blocking temperature.

In order to confirm the occurrence of EB effect in our film, the hysteresis loops of $Ni_{49.8}Mn_{36.1}Sn_{13.9}$ film were measured at various temperatures by cooling the film in presence of field from 310 K down to the required temperature of interest and then varying the field in the range ±2 T (Fig. 2). However, for clear visibility of the loop shifts from the origin, the loops are shown only in the low field range −0.6 to 0.6 T. The inset of Fig. 2(a) and (b) clearly show that the hysteresis loops shift considerably to the negative field side at low temperatures below T_B, which indicates the existence of EB in this film. The shift to the negative field side almost disappears near T_B (55 K), as shown in Fig. 2(c), and no shift is observed above T_B, as shown in inset of Fig. 2(d). The key factor in the theory of exchange bias is to understand how the coupling between the AFM and FM phases leads to a unidirectional anisotropy. The experimentally observed hysteresis loop shift indicates that the two configurations

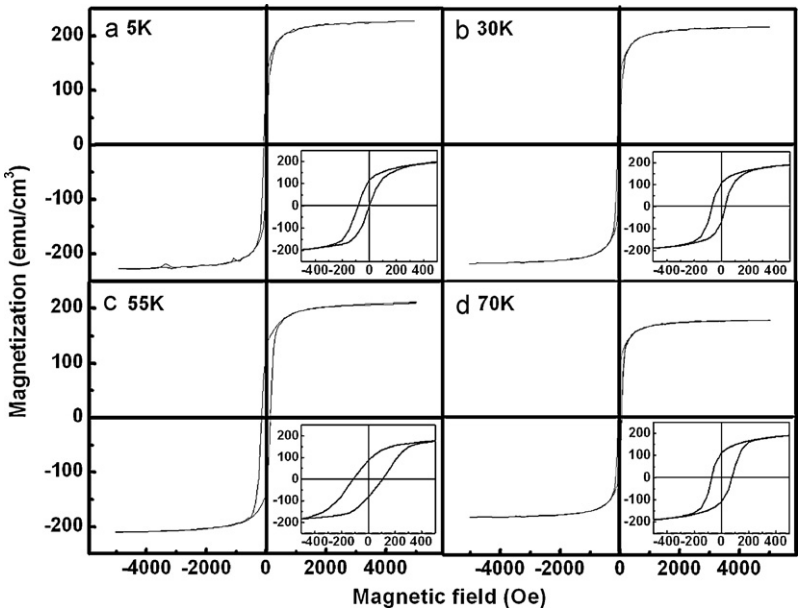

Fig. 2. Magnetization hysteresis loops of $Ni_{49.8}Mn_{36.1}Sn_{13.9}$ film measured at (a) $T = 5$ K (b) $T = 30$ K (c) $T = 55$ K and (d) $T = 70$ K. The inset shows the enlarged view of the low field region of the loops.

at the respective end points of the curve have different energies. When the interfacial layer of the AFM phase is uncompensated and is perfectly flat (free from surface defects), the existence of a coupling between the FM and AFM can be understood as the interfacial AFM spins maintain their initial relative orientations. So the initial and final configurations, before and after inversal of applied field will have different energies. For this case, Neel and Mauri et al. [25,26] separately have shown that experimental results can be matched with the theory when a domain wall forms in the AFM during the reversal of the FM magnetization. For the compensated interface plane, i.e. when there is an equal number of positive and negative exchange interactions across the interface so that the net exchange interaction vanishes, it was shown by Koon et al. [27] that due to frustration of interfacial spins, the FM magnetization will align perpendicular to the AFM easy axis. This type of coupling between the FM and the AFM is referred as spin-flop coupling. But this type of coupling does not lead to the formation of a domain wall in the AFM during FM magnetization reversal and is therefore not suitable for exchange bias. Another mechanism was given by Malozemoff et al. [28] who explained the coupling as due to a random field, which he attributed to interface roughness, and to the formation of domains in the AFM when the system is cooled through the Neel temperature. While this theory successfully explains most of the common phenomena related to exchange bias it fails to explain the tendency of the FM to align perpendicularly to the AFM easy axis. Suhl and Shuller [29] proposed another mechanism which explains the loop shift using a quantum mechanical description of the spins. They showed that the emission and reabsorption of virtual spin waves leads to exchange bias. Clearly, there are several possible mechanisms that lead to the result that the hysteresis loop unidirectionally shifts to the field axis. All the above said mechanisms are reasonably valid in some or other materials having a well defined interface between the FM and AFM phase. But in present case the FM domains are embedded in AFM matrix and AFM–FM interaction occurs at the interface of phase separation which causes a unidirectional anisotropy in the material. Therefore in our case it can be explained by the unidirectional anisotropy produced by the AFM–FM coupling at the interface of two coupled phases [30,31]. On application of magnetic field in a certain direction above Neel temperature (T_N), the FM spins get aligned in the direction of field while AFM spins remain unaffected. Below T_N, the interfacial interaction between the FM–AFM spins tries to align the AFM spins also, at the FM–AFM interface, ferromagnetically with the FM spins. When the applied field direction gets reversed, the FM spins start rotating but the AFM spins remain unchanged if the AFM anisotropy is large enough to get affected by the field rotation. Further, the AFM spins at the interface exert force on the FM spins to keep them ferromagnetically aligned and to prevent them from rotation on reversal of magnetic field direction resulting in unidirectional anisotropy of FM spins. Due to this unidirectional anisotropy, the field required to completely rotate the FM layer along its direction is larger when it is in contact with AFM spins because an additional field is needed to overcome the torque exerted by AFM spins on the FM spins at the interface, to keep them ferromagnetically aligned. However, when the field again gets reversed back to its initial direction, the FM spins gets rotated easily along the field direction at smaller value of applied field since the field applied is in the same direction in which AFM spins exert torque on the FM spins. Thus, due to this unidirectional anisotropy present in the film the hysteresis loop gets shifted along the field axis resulting in EB. Moreover, the EB effect exists in the film only at low temperatures below T_B as the AFM anisotropy responsible for EB decreases with increasing temperatures.

Fig. 3 shows variation of the exchange bias field (H_E) and coercivity (H_C) as a function of temperature for $Ni_{49.8}Mn_{36.1}Sn_{13.9}$ film. H_E and H_C are calculated using $H_E = -(H_1 + H_2)/2$ and $H_C = |H_1 - H_2|/2$, where H_1 and H_2 are the negative and positive fields at which magnetization becomes zero, respectively. The H_E decreases almost linearly with increasing temperature in the low temperature region and gradually disappears around T_B, whereas H_C first increases with increasing temperature, becomes maximum at T_B and then starts decreasing. This behaviour verifies that the exchange bias effect in $Ni_{49.8}Mn_{36.1}Sn_{13.9}$ film exists only when $T < T_B$. Such behaviour of H_E and H_c is typical for EB systems [5]. The similar behaviour was also observed in Ni–Mn–Sb [11], Ni–Mn–Sn [12] and Ni–Mn–In [13] bulk alloys. The decrease of H_E with increasing temperature is due to the fact that FM interaction begins to dominate and the AFM anisotropy decreases with increasing temperature. This result in weakening of FM–AFM interfaces coupling which is responsible for EB effect and as a result H_E decreases. Further, the lower value of H_C at low temperature is due to larger AFM anisotropy due to which

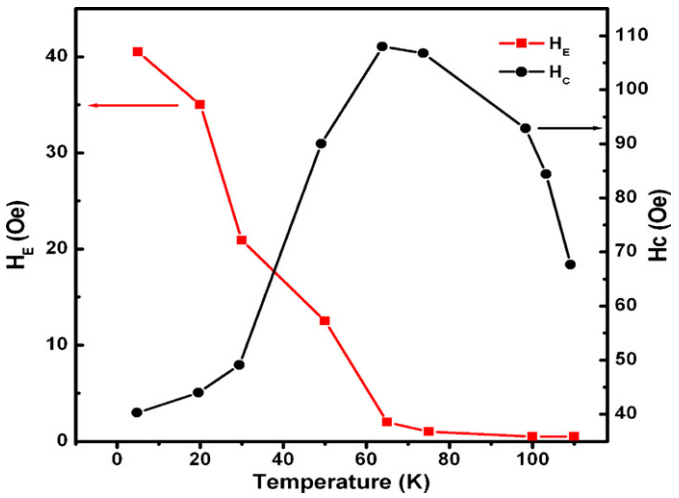

Fig. 3. Exchange bias field (H_E) and coercivity (H_C) as a function of temperature for $Ni_{49.8}Mn_{36.1}Sn_{13.9}$ film.

FM decouples because it cannot drag AFM spins. With increase in temperature, H_C increases and a peak is observed at T_B which is due to the decrease in AFM anisotropy, as a result of which the FM is able to drag more AFM spins, thus resulting in increase of H_C. Above T_B, AFM is randomly oriented and does not hinder FM rotation. Therefore, H_C reaches maximum value at T_B and then starts decreasing.

Fig. 4 shows the effect of cooling field on H_E and H_C of $Ni_{49.8}Mn_{36.1}Sn_{13.9}$ film at 5 K. The film was cooled from 310 to 5 K in different fields ranging from 10 to 50 kOe and magnetic hysteresis loops were measured in the ±10 kOe range. It is evident from the curves in Fig. 4 that H_E continuously decreases whereas H_C goes on increasing with the cooling field. The higher value of H_E at lower cooling field is due to the fact that low cooling field is insufficient for the complete saturation of the FM region. Therefore, the alignment of the FM region increases along a certain direction which results in increase in interaction at the FM/AFM interface due to exchange coupling. This leads to larger value of H_E at low cooling field. Further, the decrease in H_E in high cooling fields is due to the complete alignment and growth of the FM regions due to which EB decreases, since EB is inversely proportional to the thickness of the FM layer

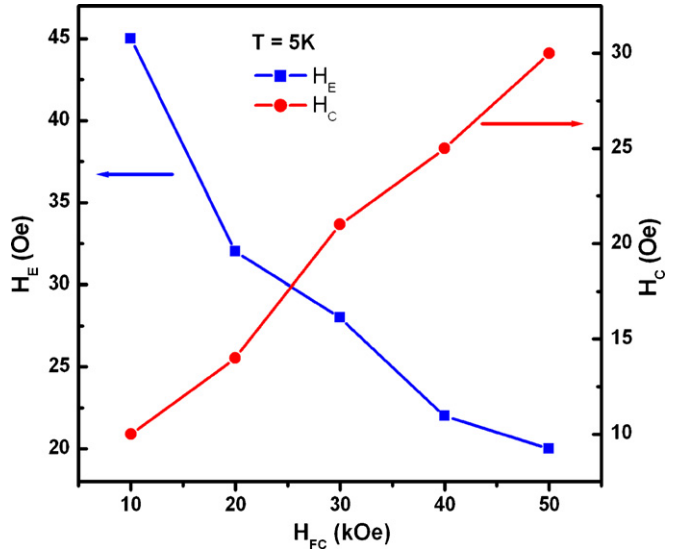

Fig. 4. Variation of EB field (H_E) and coercivity (H_C) with the cooling field (H_{FC}) for $Ni_{49.8}Mn_{36.1}Sn_{13.9}$ film at 5 K.

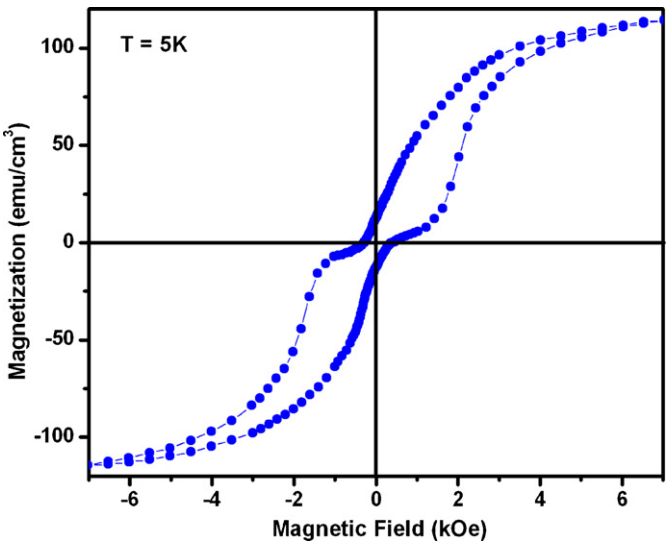

Fig. 5. Magnetic hysteresis loop of $Ni_{49.8}Mn_{36.1}Sn_{13.9}$ film obtained in ZFC mode at 5 K.

[3] and as a result H_E also decreases. The increase in H_C of film with increase in cooling field is due to change in AFM anisotropy with field. As cooling field increases, AFM anisotropy decreases and FM is able to drag more AFM spins, thus increasing the coercivity.

The shape of magnetic hysteresis loop is ascribed to the internal material parameters. A noteworthy feature observed in material showing exchange bias is the occurrence of double-shifted hysteresis loop. When system is cooled under zero field condition, instead of exhibiting a single hysteresis loop it exhibits a loop that is divided into two subloops, one subloop is shifted to positive field and other to the negative field. This type of hysteresis loop is generally called "double-shifted hysteresis loop". Fig. 5 shows the double shifted ZFC hysteresis loop which further confirms the presence of EB effect in the film. Such double shifted loop observed in ZFC state is usually observed in EB materials in which AFM–FM coupling coexist [32]. The occurrence of this double shifted loop is due to the division of AFM region during ZFC into two regions locally oriented in opposite directions that are equally preferred. During magnetization measurement each of these regions couple in opposite manner to the FM regions, resulting in double shifted hysteresis loop [11]. The occurrence of double shifted loop in $Ni_{49.8}Mn_{36.1}Sn_{13.9}$ film could also be explained by exchange-spring effects [33]. According to this effect, the AFM regions form a continuous matrix in which FM regions get embedded in the form of clusters. This results in significant exchange at the interface that leads to the alignment of FM spins by AFM spins. The cluster spin orientation is set either up or down resulting in double shifted loop.

4. Conclusion

In conclusion, we have observed the EB effect in the martensitic state of $Ni_{49.8}Mn_{36.1}Sn_{13.9}$ film. Shift in hysteresis loops of up to 41 Oe was observed in the 2 T field cooled film. Both H_E and H_C are found to strongly depend on temperature. The observed EB behaviour in $Ni_{49.8}Mn_{36.1}Sn_{13.9}$ film at low temperatures below T_B is attributed to the unidirectional anisotropy which arises due to the coupling between AFM and FM interactions in the martensite phase of the film. The double shifted hysteresis loop observed at 5 K during ZFC, confirms the existence of EB effect in the film at low temperature. This study gives a possibility of application of Ni–Mn–Sn FSMA films for device applications since most of the applications based on EB effect are in thin film form.

Acknowledgements

The financial support provided by Department of Information Technology (DIT), India under Nanotechnology Initiative Program with reference no. 20(11)/2007-VCND is highly acknowledged. The author, Ritu Vishnoi, is thankful to MHRD for the award of senior research fellowship.

References

[1] W.H. Meiklejohn, C.P. Bean, Phys. Rev. 102 (1956) 1413.
[2] J.C.S. Kools, IEEE Trans. Magn. 32 (1996) 3165.
[3] J. Nogues, I.K. Schuller, J. Magn. Magn. Mater. 192 (1999) 203.
[4] J. Nogues, J. Sort, V. Langlais, V. Skumryev, S. Surinach, J.S. Munoz, M.D. Baro, Phys. Rep. 422 (2005) 65.
[5] A.E. Berkowitz, K. Takano, J. Magn. Magn. Mater. 200 (1999) 552.
[6] S. Velthuis, G. Felcher, J. Jiang, A. Inomata, C. Nelson, A. Berger, S. Bader, Appl. Phys. Lett. 75 (1999) 4174.
[7] E. Arenholz, K. Liu, Z.P. Li, I.K. Schuller, Appl. Phys. Lett. 88 (2006) 072503.
[8] M. Wuttig, L.H. Liu, K. Tsuchiya, R.D. James, J. Appl. Phys. 87 (2000) 4707.
[9] K. Ullakko, J.K. Huang, C. Kantner, R.C. O'Handley, V.V. Kokorin, Appl. Phys. Lett. 69 (1996) 1966.
[10] T. Krenke, M. Acet, E.F. Wassermann, X. Moya, L. Manosa, A. Planes, Phys. Rev. B 72 (2005) 014412.
[11] M. Khan, I. Dubenko, S. Stadler, N. Ali, Appl. Phys. Lett. 91 (2007) 072510.
[12] Z. Li, C. Jing, J. Chen, S. Yuan, S. Cao, J. Zhang, Appl. Phys. Lett. 91 (2007) 112505.
[13] B.M. Wang, Y. Liu, L. Wang, S.L. Huang, Y. Zhao, Y. Yang, H. Zhang, J. Appl. Phys. 104 (2008) 043916.
[14] S.B. Roy, M.K. Chattopadhyay, P. Chaddah, Phys. Rev. B 71 (2005) 174413.
[15] A.K. Nayak, K.G. Suresh, A. K Nigam, J. Phys. D: Appl. Phys. 42 (2009) 035009.
[16] S. Majumdar, E.V. Sampathkumaran, P.L. Paulose, H. Bitterlich, W. Löser, G. Behr, Phys. Rev. B 62 (2000) 14207.
[17] R. Vishnoi, D. Kaur, J. Appl. Phys. 107 (2010) 103907.
[18] R. Vishnoi, D. Kaur, Surf. Coat. Tech. 204 (2010) 3773.
[19] K. Bhattacharya, R.D. James, J. Mech. Phys. Solids 47 (1999) 531.
[20] J.W. Dong, J.Q. Xie, J. Lu, C. Adelmann, C.J. Palmstrom, J. Cui, Q. Pan, T.W. Shield, R.D. James, S. Mckernan, J. Appl. Phys. 95 (2004) 2593.
[21] P. Singh, D. Kaur, J. Appl. Phys. 103 (2008) 043507.
[22] A. Kumar, D. Singh, D. Kaur, Talanta 78 (2009) 964.
[23] P.J. Brown, A.P. Gandy, K. Ishida, R. Kainuma, T. Kanomata, K.U. Neumann, K. Oikawa, B. Ouladdiaf, K.R.A. Ziebeck, J. Phys.: Condens. Matter 18 (2006) 2249.
[24] P.A. Bhobe, K.R. Priolkar, P.R. Sarode, J. Phys.: Condens. Matter 20 (2008) 015219.
[25] L. Neel, Ann. Phys. (Paris) 2 (1967) 61.
[26] D. Mauri, H.C. Siegmann, P.S. Bagus, E. Kay, J. Appl. Phys. 62 (1987) 3047.
[27] N.C. Koon, Phys. Rev. Lett. 78 (1997) 4865.
[28] A.P. Malozemoff, et al., Phys. Rev. B 35 (1987) 3679;
A.P. Malozemoff, et al., Phys. Rev. B 37 (1988) 7673;
A.P. Malozemoff, et al., J. Phys. Rev. 63 (1988) 9874.
[29] H. Suhl, I.K. Schuller, Phys. Rev. B 58 (1998) 258.
[30] W.H. Meiklejohn, J. Appl. Phys. 33 (1962) 1328.
[31] N.H. March, P. Lambin, F. Herman, J. Magn. Magn. Mater. 44 (1984) 1.
[32] S. Bruck, J. Sort, V. Baltz, S. Surinach, J.S. Munoz, B. Dieny, M.D. Baro, J. Nogues, Adv. Mater. (Weinheim. Ger.) 17 (2005) 2978.
[33] A.N. Dobrynin, M.J. Van Bael, K. Temst, P. Lievens, New J. Phys. 9 (2007) 258.